

Published in final edited form as:

Nat Protoc. 2010 February ; 5(2): 247–254. doi:10.1038/nprot.2009.228.

Targeted optogenetic stimulation and recording of neurons *in vivo* using cell-type-specific expression of Channelrhodopsin-2

Jessica A Cardin^{1,2,7}, Marie Carlén^{3,4,7}, Konstantinos Meletis^{3,4}, Ulf Knoblich¹, Feng Zhang⁵, Karl Deisseroth⁵, Li-Huei Tsai^{3,4,6}, and Christopher I Moore¹

¹McGovern Institute for Brain Research and Department of Brain and Cognitive Sciences, MIT, Cambridge, Massachusetts, USA

²Department of Neuroscience, University of Pennsylvania, Philadelphia, Pennsylvania, USA

³Picower Institute for Learning and Memory, Department of Brain and Cognitive Sciences, MIT, Cambridge, Massachusetts, USA

⁴Stanley Center for Psychiatric Research, Broad Institute of Harvard and Massachusetts Institute of Technology, Cambridge, Massachusetts, USA

⁵Department of Bioengineering, Stanford University, Stanford, California, USA

⁶Howard Hughes Medical Institute, Cambridge, Massachusetts, USA

Abstract

A major long-term goal of systems neuroscience is to identify the different roles of neural subtypes in brain circuit function. The ability to causally manipulate selective cell types is critical to meeting this goal. This protocol describes techniques for optically stimulating specific populations of excitatory neurons and inhibitory interneurons *in vivo* in combination with electrophysiology. Cell type selectivity is obtained using Cre-dependent expression of the light-activated channel Channelrhodopsin-2. We also describe approaches for minimizing optical interference with simultaneous extracellular and intracellular recording. These optogenetic techniques provide a spatially and temporally precise means of studying neural activity in the intact brain and allow a detailed examination of the effect of evoked activity on the surrounding local neural network. Injection of viral vectors requires 30–45 min, and *in vivo* electrophysiology with optogenetic stimulation requires 1–4 h.

INTRODUCTION

One of the main goals of systems neuroscience is to understand the architecture and function of neural circuits. These circuits consist of a complex network of varying neural subtypes. In the cortex and hippocampus, local neural circuits are comprised of excitatory neurons, which are often pyramidal cells, and several classes of inhibitory interneurons^{1–5}. The development of technologies to regulate the activity of specific types of cells is key to understanding how they contribute to local network activity and overall brain function *in vivo*. This control has recently become feasible with the advent of optogenetics, the optical

© 2010 Nature Publishing group

Correspondence should be addressed to C.I.M. (cim@mit.edu), L.-H.T. (lhtsai@mit.edu) and/or K.D. (deissero@stanford.edu).

⁷These authors contributed equally to this work.

AUTHOR CONTRIBUTIONS F.Z. and K.D. designed and cloned the AAV DIO ChR2-mCherry vector; M.C. and K.M. characterized the virus *in vitro* and *in vivo* and injected the animals; M.C. performed histological analyses; J.A.C. developed the experimental paradigm, and performed and analyzed the extracellular recordings; U.K. and J.A.C. performed the intracellular recordings; U.K. analyzed the intracellular data; and J.A.C., M.C., K.M., U.K., L.-H.T., and C.I.M. wrote the paper.

control of neural activity by artificial incorporation of light-sensitive proteins into cell membranes. This approach provides a reliable method for stimulating neural activity in mammalian tissue *in vitro*^{6–8} and *in vivo*^{9–15}. The use of optogenetic tools to stimulate or suppress the activity of neural populations has potential applications for both experimental and therapeutic approaches. Recent studies have highlighted the use of cell-type-specific expression of the light-sensitive cation channel Channelrhodopsin-2 (ChR2), which is activated by ~470 nm light, as a tool for exploring the functional role of inhibitory interneurons in gamma oscillations in the intact brain¹² and information processing *in vitro*⁸.

Previous experiments¹² required efficient viral transduction, cell-type-specific expression of light-sensitive channels and *in vivo* integration of optical stimulation with extracellular and intracellular recording techniques. This paper was one of the first to realize the promise of optogenetics to test hypotheses about the roles of specific neural populations in the *in vivo* mammalian neocortex. Because there is broad interest in applying this approach *in vivo* to the cortex or closely related systems, such as the hippocampus, we provide here a detailed description of methods.

Combined optical stimulation and electrophysiological recordings *in vivo*

The use of light activation for assessing neural network dynamics requires simultaneous application of neural recording techniques and extrinsic network modulation. One specific challenge raised by this combination is that optical stimulation can induce various electrical artifacts during such recordings. These artifacts could emerge from causes ranging from possible photoelectric effects to temperature-dependent effects on electrode conduction properties. These challenges have proven relatively easy to circumvent *in vitro* but have interrupted effective recording of field potentials—the most commonly used marker for cortical dynamics—in recent optogenetic studies *in vivo*¹³. This protocol describes optically induced artifacts in the mouse neocortex and outlines means for minimizing their impact.

Cell-type-specific expression of light-activated channels

A variety of approaches can be used to achieve insertion of light-activated elements into neurons that are otherwise not optically sensitive, including constitutive expression in transgenic mice¹⁶, *in utero* electroporation¹⁴ and use of viral approaches both with and without associated use of a Cre-loxP system^{8,11,12}. These methods have strengths and weaknesses in generating cell-type-specific expression. Generation of transgenic mice expressing cell-type-specific ChR2 is effective¹⁴, but costly and time-consuming. *In utero* electroporation can be targeted to general cell classes by varying the site and prenatal day of treatment^{17–22}. This early surgery has the advantage of allowing maximal recovery of the pups across development and of providing at least some cell-type specificity in any given model species. However, this approach requires an invasive surgery *in utero* in which probes are inserted into the fetal brain, which can have negative scientific and practical implications for a given experiment. Most importantly, cell-type specificity of expression is limited to the resolution provided by knowledge of cell birth date and relatively broad localization to the targeted germinal zones²³.

The most commonly used strategy to date for the expression of ChR2 in brain tissue is through viral transduction. Viral vectors driving ChR2 expression can be delivered directly into specific brain regions with robust transduction efficacy and limited tissue damage. Adeno-associated viruses (AAVs) provide extensive spatial spread and high expression levels^{12,24}. Lentiviral vectors expressing light-activated channels have also been used in the cortex but do not appear to spread as effectively as AAV vectors^{7,13–15}. Further, recent evidence suggests that lentiviruses preferentially transduce excitatory neurons²⁵ and thus

appear to be applicable for targeting this cell population but may not be suitable for targeting inhibitory interneurons.

Targeted expression of genes to specific cell types can be robustly achieved with the Cre-loxP system. Recent studies have used 'double-floxed' inverted open reading frame (DIO) viral vectors to achieve high specificity and expression levels^{8,11,12,26}. We have recently used the viral vector AAV DIO-ChR2-mCherry (AAV DIO ChR2-mCherry) in knock-in and transgenic Cre mice to target the expression of ChR2 to defined neuronal populations (Fig. 1a)¹². In AAV DIO ChR2-mCherry, two incompatible loxP variants flank an inverted version of ChR2 fused to the fluorescent marker mCherry. In the presence of Cre, a stochastic recombination of either loxP variant takes place²⁷, resulting in the inversion of ChR2-mCherry into the sense direction, followed by expression of the light-activated channels. Cre-dependent expression of light-activated channels or other genes is particularly well suited for targeting expression to cell types that lack identified promoter sequences. In most cases, cellular promoters are not yet identified or are incompatible for use in viruses because of size limitations. Cellular promoters may also fail to render enough specificity or sufficient expression levels for meaningful optogenetic studies.

Successful use of optogenetic techniques relies on sufficient expression levels of the light-activated channels, which limits the use of small promoter elements⁸. To circumvent issues of specificity and expression levels, the vector AAV DIO ChR2-mCherry depends on a strong and general promoter (EF1 α , elongation factor 1 α), and cell-type specificity is conferred by the unique Cre expression pattern of each transgenic mouse line^{8,11,12}. The inverted strategy of AAV DIO ChR2-mCherry eliminates the need for a polyadenylation stop-cassette in the viral construct, as the presence of Cre followed by recombination is needed for inversion of ChR2-mCherry into the sense direction, leading to expression of the opsin. For a thorough explanation of the double-floxed inverted strategy, see reference 12.

Traditionally, Cre-dependent viral vectors are constructed with a loxP-flanked transcriptional stop cassette preceding the gene of interest, but the size limitations of the viral vectors exclude the use of large stop cassettes. As a result, only smaller stop cassettes are possible in viral vectors, leading to documented leakiness and expression of the gene of interest in the absence of Cre^{6,8}.

The application of optogenetics to *in vivo* electrophysiology has opened up an unprecedented possibility for analysis of neural circuits by the characterization of cell-type-specific functions. The combination of several publicly available mouse lines with Cre expression in defined neuronal populations with AAV viruses conferring Cre-dependent expression of light-activated channels provides a new experimental framework for the detailed characterization of activity in the intact brain. The techniques described here provide an approach for navigating the many challenges of cell-type-specific targeting, successful viral delivery and uncontaminated electrophysiological recording during optical stimulation, and may be used to facilitate studies of the role of specific cell types in mammalian brain function.

Experimental design

Cell type targeting, expression construct and virus—The use of a viral DIO construct allows for expression of ChR2 exclusively in the subpopulation of neurons that expresses Cre recombinase. A number of transgenic, BAC and knock-in mouse lines, now commercially available, express Cre in specific populations of excitatory neurons (e.g., CW2, T29-1, T29-2, respectively) or inhibitory interneurons (e.g., PV-Cre). The specificity of ChR2 expression conferred by the DIO construct is very high (Fig. 1b,c)^{8,11,12}. However, individual Cre lines exhibit varying degrees of cell-type-specific Cre expression, which can

result in the expression of ChR2 in mixed neuronal populations. A fluorescent tag, such as mCherry fused to ChR2, allows *post-hoc* identification and mapping of ChR2-expressing cells for direct assessment of the specificity of expression (Fig. 1b,c). Control injections of the floxed viral construct should be made in mice that do not express Cre recombinase to confirm that the expression of ChR2-mCherry does not occur.

The selection of a viral vector is important, as different viruses and virus serotypes exhibit different cellular tropisms^{28–31}. Both AAV^{8,10–12} and lentivirus^{7,13–15} have been successfully used for expression of light-activated channels in several brain areas, including the cortex and hippocampus. In addition, the degree of viral spread from the injection site can vary widely with virus²⁹ and tissue type transduced²⁴. One advantage of AAV is the broader spatial spread of ChR2 expression around the injection site. We routinely observe expression over a distance of up to 2 mm of cortical tissue (Fig. 1b)¹². The protocol outlined here specifies the use of an AAV vector, but may be successfully used with other virus types.

Injection parameters—Slow injection of small volumes of virus is critical for effective transduction of neural tissue with minimal damage. The post-injection wait time sufficient for maximal expression levels of ChR2 varies with virus type. We have observed high levels of ChR2 6 d after cortical injection of AAV DIO vectors¹², with expression remaining high for at least several months after the initial injection.

Electrophysiology—Single extracellular electrodes or multielectrode arrays may be placed several hundred microns away from the injection site, ensuring that the recordings are made from transduced tissue that is undamaged by the initial viral delivery (Fig. 2a–c). Similarly, ChR2 stimulation works well in conjunction with intracellular recordings *in vivo* (Fig. 2d). The latency to light-evoked spikes and the precision of evoked spike timing will vary with cell type, region of the cell stimulated (e.g., soma versus axon) and light stimulus intensity¹². In addition, for anesthetized experiments, physiological state should be monitored by several means including simultaneous electroencephalogram recording, as the effects of light stimulation on spike rate and local field potential (LFP) signals will vary with anesthesia depth. Direct laser light on metal electrodes can cause electrical artifacts that obscure LFP signals, but these can be reduced by several measures (see TROUBLESHOOTING and Fig. 3). Control recordings should be made from untransduced tissue to confirm that light-evoked neural activity is only observed in tissue expressing ChR2.

Light stimulation parameters—Light spreads in an approximate cone from the point source at the tip of the optical fiber, and light power from a fiber at the surface of the brain decreases with tissue depth³². Light intensity is usually measured in mW mm^{-2} , and a safe range for *in vivo* experiments is up to $\sim 75 \text{ mW mm}^{-2}$ for short pulses (~ 0.5 to 50 ms). We have observed significant tissue damage in the cortex immediately under the optical fiber from sustained stimulation (>500 ms duration) at levels above 100 mW mm^{-2} . Light can be applied through the mouse dura or thinned skull, and surface positioning of the optical fiber allows effective stimulation throughout supragranular and granular cortical layers in the mouse sensory cortex ($\sim 500 \mu\text{m}$ depth). Alternatively, optical fibers of smaller diameter (50 – $100 \mu\text{m}$) can be placed in the brain for stimulation of deeper cells or smaller volumes of tissue. It is important to consider the duration and strength of the light pulse, as continuous light application can cause abnormal levels of neural activity and excitotoxicity. Power transmitted by the fiber will vary with fiber type (multimode or single-mode) and the spread of light from the fiber is partially determined by the numerical aperture (NA), with low NA corresponding to a narrow angle and high NA corresponding to a larger angle. Power delivered to the tissue (in mW mm^{-2}) will also vary with the radius (r) of the fiber, as the

area of the initial cross-section of the light at the tip of the fiber increases as πr^2 . Power decreases with distance from the light source³², giving varying effective intensities at different cortical depths.

MATERIALS

REAGENTS

- Experimental animals (mice) ! **CAUTION** Use of live rodents must conform to national and institutional rules and regulations.
- AAV of desired serotype at titer of $\sim 10^{12}$ (can be stored for ~ 1 year at -80 °C)
- Dye marker (Fast Green 2.5%, Electron Microscopy Sciences, cat. no. 26364-05)
- Sterile saline (NaCl 0.9%, Henry Schein, cat. no. 1200721)
- Anesthetic (Isoflurane, Henry Schein, cat. no. 2091966)
- Local anesthetic (Lidocaine 1%, Henry Schein, cat. no. 2586460)
- Analgesic (Buprenorphine, Henry Schein, cat. no. 1048721)
- Iodine-based wash (Betadine, Henry Schein, cat. no. 6906950)
- Cyanoacrylate glue (Vetbond Tissue Adhesive, Henry Schein, cat. no. 7003449)
- Eye lubricant (Puralube Ointment, Henry Schein, cat. no. 4725942)
- Mineral Oil (White, Light, Fisher Scientific, cat. no. O121-1)
- Tank of compressed O₂

EQUIPMENT

- Isoflurane vaporizer (Harvard Apparatus, cat. no. 728130)
- Stereotaxic frame with anesthesia head holder and arms for electrode holders (David Kopf, Model no. 930, Model no. 1760-61, Model no. 1460 and Model no. 923-B)
- Stereotaxic injector system (Stoelting QSI, Stoelting, cat. no. 53311)
- Heating blanket (Harvard Apparatus, cat. no. 507220F)
- Surgical tools (Fine Science Tools)
- Microfiles (26g MicroFil, World Precision Instruments, cat. no. CMF26G6L)
- High-speed dental drill (Classic High-Speed Handpiece, Johnson- Promident)
- Drill bits (Johnson-Promident, cat. no. 1/4FG)
- Hair trimmer (Harvard Apparatus, cat. no. 525204)
- Pipette Puller (Sutter Instrument, Sutter Model P-97)
- Electrophysiology equipment for extracellular or intracellular recordings
- Extracellular electrodes (e.g., single tungsten electrodes, FHC; prefabricated tetrode arrays, NeuroNexus Technologies; or twisted wire stereotrodes or tetrodes)
- Graduated borosilicate glass capillaries (Wiretrol I, Drummond; Calibrated Micropipette, 10 μ l size, Fisher Scientific)
- ~ 473 nm laser (e.g., Opto Engine LLC or IkeCool)

- Breadboard (1/2" Solid Aluminum Breadboard, Thorlabs, part no. MB1824)
- Posts (Thorlabs; 1/2" posts)
- FiberPort Coupler (FiberPort, part no. PAF-SMA-5-A and HCP-L Bracket Mount; Thorlabs)
- Optical Fiber (Thorlabs, BFH22-200 or BFH37-200)
- SMA connectors (Fiber SMA Connectorization Kit, SMA 905 connectors, Thorlabs)
- Optical power meter (PM100D power meter, S120C power sensor, NE03A optical density filter, Thorlabs)

REAGENT SETUP

Virus—Add a small amount (~0.05 to 0.1 μl) of Fast Green to 1 μl of the virus solution.

EQUIPMENT SETUP

Surgical tools—For injection surgeries, tools and workspace should be sterilized according to institutional procedures.

Injection pipettes—Glass injection pipettes should be pulled to have a shank of several millimeters and a relatively sharp tip with a diameter of ~40 to 80 μm . Using a syringe and a MicroFil, the pipette should be completely filled with mineral oil to the tip. Break the tip back slightly with forceps or scissors to allow free flow of the oil.

Stereotaxic setup—At least two manipulators are necessary: one to hold the recording electrodes and another to position the optical fiber. For extracellular recordings, these can both be fairly coarse, but intracellular recordings require high-resolution manipulators with specialized pipette holders. The animal should be firmly placed in the stereotaxic apparatus, with the head appropriately positioned for the precise use of landmarks for injections and recordings. Connect the output of the isoflurane vaporizer to the input on the anesthesia head holder.

Anesthesia setup—The animal should be anesthetized initially with a small dose of isoflurane administered in an induction chamber or small container, as determined by institutional policy. The animal should then be placed in the stereotaxic frame with the nose in the anesthesia head-holder with (at ~0.5 to 1 liter min^{-1}) running to the apparatus. Initial isoflurane in O_2 isoflurane levels after induction may be as high as 2% and may be lowered over the course of surgery to ~1% as the animal reaches a stable plane of anesthesia.

Optics setup—The laser and optics parts should be stably attached to the breadboard so that the laser beam hits the center of the fiberport. An SMA connector should be attached to the optical fiber of the desired core diameter and the fiber should then be connected to the output connector on the fiber port. Before starting any stimulation, the input–output function of the laser should be tested with the optical power meter. Many lasers produce variable light output depending on voltage input, and it is important to carefully calibrate the light intensity at the tip of the fiber (mW mm^{-2}) at each input voltage level. Only a low total output power may be needed to achieve ChR2 activation. For instance, 2 mW at the tip of a 200- μm core diameter fiber corresponds to 63.7 mW mm^{-2} , well above the minimal effective range for *in vivo* stimulation. Mount the fiber on an electrode manipulator for positioning in the craniotomy (Fig. 2a).

PROCEDURE

Virus injection • TIMING 30–45 min

- 1| Anesthetize the animal and place it in the stereotaxic apparatus on a heating blanket (37 °C) in a sterile surgical environment.
▲ CRITICAL STEP Test the animal's reflexes to determine that a surgical level of anesthesia has been reached before proceeding with surgery.
- 2| Using hair trimmers, shave the scalp above the area of interest.
- 3| Raise the skin with forceps and administer several small subcutaneous injections of lidocaine or a similar local anesthetic. Wait 2–3 min for injections to take effect.
- 4| Using a fresh scalpel blade, make a single incision through the skin. Ensure that the incision runs far enough along the anterior–posterior axis to expose stereotaxic markers. Gently push aside connective tissue on top of the skull as needed for clear viewing.
- 5| Using stereotaxic coordinates, mark the intended site of virus injection.
- 6| Make a single burr-hole in the skull with the drill at the injection site. Stop when the drill bit reaches the bottom of the skull. The total diameter of the burr hole should be no more than 100 μm . A thin layer of skull may remain. Using a syringe needle, remove a small piece of any remaining skull so that the dura can be seen. The opening in the dura should be not more than several tens of microns in diameter. Flush the site with sterile saline while drilling to remove bone dust and control heat generation.
▲ CRITICAL STEP Too much pressure can cause the drill to penetrate too far and directly damage the dura and underlying tissue, causing cellular degeneration post-injection. The drill head should never touch the dura.
- 7| Fill the tip of the injection pipette with $\sim 1 \mu\text{l}$ of virus tinted with Fast Green and position the pipette over the burr hole. Lower the pipette until the tip touches the exposed dura and use this point as the 'zero.' Lower the pipette tip through the dura to the desired depth in the brain tissue.
- 8| Inject virus at a rate of not more than $0.1 \mu\text{l min}^{-1}$. When the injection is completed, allow a minimum of 10 additional minutes rest time before beginning to retract the pipette from the brain. Retract the pipette slowly, in two stages, allowing another 5 min rest time at the halfway point.
▲ CRITICAL STEP Injecting virus rapidly or withdrawing the pipette too fast can cause the fluid to flow out of the injected site up the track, reducing the effective volume.
▲ CRITICAL STEP Using the Fast Green as a marker, ensure that the correct volume of virus is expelled through the pipette.
- 9| Pull the edges of the skin together and clean lightly with Betadine. While holding the edges of the incision together, apply small amounts of cyanoacrylate glue to seal. The burr hole does not need to be covered or filled.
- 10| Allow the animal to recover from the anesthetic and treat with analgesic (e.g., Buprenorphine) for at least 3 d after injection surgery.

■ **PAUSE POINT** For neocortical and hippocampal injections in PV-Cre and CW2-Cre mice, 6 d after injection was sufficient delay to produce effective expression levels of ChR2 in interneurons and excitatory neurons, respectively. Longer wait times will allow for higher expression of ChR2 and may be necessary for a desired expression level in other brain areas.

Stimulation and recording of ChR2-expressing neurons • TIMING 1–4 h

- 11| Anesthetize the animal and give local anesthetic as in Steps 1 and 3. Using forceps, remove any remaining cyanoacrylate glue from the skin. Reapply local anesthetic throughout the experiment.
- 12| Using the initial burr hole as a marker, make a clean craniotomy next to the injection site. One side of the craniotomy may abut the injection site, but the targeted area for recording should be at least 200 μm away from the injection site to reduce the potential for recording from damaged tissue. The craniotomy should be large enough to allow positioning of both the optical fiber and the electrodes.

▲ **CRITICAL STEP** Disrupting the dura or causing direct brain tissue damage with the drill will result in bleeding, obscuring the placement of electrodes and reducing laser light transmission.

- 13| Make a small incision in the dura to allow the placement of electrodes, being careful to not cause bleeding. This opening can be accomplished with a fine syringe tip (29 gauge), fine forceps or fine scissors. Lightly tapping a fine syringe tip orthogonal to a hard surface can produce a hook that can facilitate snagging the dura.
- 14| Place the extracellular electrodes in the brain tissue at the desired angle (Figs. 2a and 3c) and depth by lowering slowly. If using an array of electrodes or a large single electrode, allow tissue to recover from electrode placement for up to 30 min before stimulating or recording. (If using intracellular electrodes, perform Step 15 first.)
- 15| Place the optical fiber close to the electrodes so that the cut surface of the bare fiber is flat against the surface of the dura. Ensure that there is no blood between the fiber ending and the dura.
- 16| Give short light pulses (~1 to 10 ms duration at 20–70 mW mm^{-2}) to evoke activity from ChR2-expressing cells (Figs. 2b and 3b,c).

? TROUBLESHOOTING

• TIMING

Steps 1–10, virus injection: ~30 to 45 min

Steps 11–16, stimulation and recording of ChR2-expressing neurons: ~1 to 4 h

? TROUBLESHOOTING

No light-evoked activity (Step 16)

1. Ensure that ChR2 is being expressed by performing histology. Identify cells expressing light-activated channels by the presence of the fluorescent protein fused to ChR2 (Fig. 1b,c).
2. Viral transduction does not always spread evenly around the injection site. We have observed a larger anteroposterior than mediolateral spread when using an AAV

DIO vector in somatosensory cortex. Move electrodes and optical fiber in small (~20 to 50 μm) steps around the injection site.

3. Light levels may not be sufficient to evoke activity. Test the light power at the end of the optical fiber to make sure that sufficient light is penetrating the brain. Ensure that the bare end of the fiber is cut cleanly and is not obscured by blood.
4. If the targeted cell type is sparsely represented in the tissue, a careful search may be necessary to find ChR2-expressing cells.
5. ChR2-expressing cells may be located too deep to stimulate with an optical fiber placed at the surface of the brain. In this case, a small diameter optical fiber can be lowered into the brain tissue in the same manner as an electrode. Take care to minimize bleeding, as blood can reduce laser light transmission.

Electrical artifacts (Step 16)

Several studies^{12,13,33} have recently reported electrical artifacts produced by the laser beam striking metal (Fig. 3). These effects can result from laser light hitting the tip of a metal electrode, a ground electrode or a silver wire in a glass pipette and are proportional in size to the total laser power and the amount of exposed metal. The artifacts differ from evoked neural activity, in that their onset is exactly aligned with the light onset (Fig. 3a, inset), rather than showing a delay of several milliseconds. In addition, light-induced artifacts typically show an onset ramp that continues for the duration of a stimulus if that stimulus is short (e.g., 1 ms) and have a slower offset time constant (e.g., 2–10 ms decay time in response to a 1-ms light pulse). These artifacts can contaminate both LFP recordings and intracellular traces.

Several strategies can be used to minimize optical contamination of electrophysiological recording *in vivo*. The primary goal is to limit metal exposure to light by limiting the duration of the light pulse and minimizing the total exposed metal surface. These light-mediated artifacts have relatively little impact on extracellular action potential signals and are a less significant issue if neither field potential nor intracellular recordings are needed¹³.

If field potential or intracellular signals are desired, one optimal approach is to use glass electrodes with a more distal metal wire insert that is not contacted by the light, a strategy typically used in slice or culture recordings. For field potential recordings made with glass electrodes, further adding a non-reflective, opaque coating to the glass will reduce light transmission to the silver wire in the electrode (Fig. 3a,b). We have found both non-reflective acrylic paint and nitrocellulose-based lacquers to be effective in blocking light transmission and completely eliminating measurable optical artifacts. Although this solution is useful, many *in vivo* applications require metal electrodes, as they are more optimal for chronic recording and more typically used for recordings requiring placement of multiple sites in close proximity (e.g., stereotrodes or tetrodes). We have found that tungsten electrodes with small exposed tip surfaces (e.g., twisted wire stereotrodes or tetrodes with wire diameters < 20 μm) show smaller optically induced artifacts than do tungsten electrodes with larger exposed metal tips (e.g., standard electrodes from FHC). In simultaneous local field recordings, optically induced artifacts on twisted wire stereotrodes (12.5 μm wire diameter) were $84.6 \pm 16.3\%$ smaller than those on adjacent commercially produced single electrodes (FHC tungsten electrode, 75 μm diameter, standard fine tip).

A further key step is to adjust the relative orientation of the light source and the electrode. Attaching an optical fiber directly to a metal electrode in parallel is advantageous for many deep brain optogenetic stimulation experiments. This configuration provides an ideal approach for guiding the optical stimulation to be directly above the recorded neuron or

circuit, and can allow a stiff electrode to provide a mechanical guide for fiber optic insertion. However, this approach has the drawback of adding unnecessary light exposure to the portion of the electrode shank that is transmitting the signal and thereby enhancing artifacts. Complete or near-complete eradication of artifacts can be achieved when using thin wire stereotrode or tetrodes by adjusting the angle of the electrodes so that minimal laser light strikes them directly (Fig. 3c). Preliminary data from our experiments suggest that bipolar electrode recordings may also eliminate small amplitude optical artifacts by allowing subtraction of signals generated close to the electrode tips.

Tissue damage (Step 16 and *post-hoc* analysis)

Very high light power may cause tissue damage, which can be observed *post hoc* as a compressed area in the tissue at the site of light stimulation. We have observed damage to superficial cortical tissue as a result of sustained light stimulation $>100 \text{ mW mm}^{-2}$. However, light intensities $< 75 \text{ mW mm}^{-2}$ are sufficient to evoke spike activity. In addition, tissue damage can be minimized using short light pulses rather than continuous illumination.

ANTICIPATED RESULTS

With careful injection parameters, viral transduction should give close to 100% efficacy in generating populations of neurons expressing ChR2 in each injected mouse. Because AAV-mediated ChR2 expression spreads up to several millimeters, this system works well for preparations using combined intracellular and extracellular recordings or large extracellular arrays *in vivo*. Using the AAV DIO ChR2-mCherry vector ensures 97–100% cell-type specificity of ChR2 expression, depending on the Cre line used¹². This high level of fidelity is critical for experiments whose goal is to determine the role of specific neural populations in brain function. Viral transduction should produce robust ChR2 expression levels sufficient to ensure that single light pulses of 0.5 ms duration evoke a minimum of one action potential from transduced neurons. Short light pulses will evoke initial spikes with millisecond-level precision. Frequency following at higher frequencies depends in part on cell type¹², but at lower frequencies most ChR2-expressing cells will reliably spike in response to each light pulse.

Acknowledgments

We thank members of the Tsai and Moore laboratories for discussions and comments on the paper and M.J. Higley for help with optics. This study was supported by grants to C.I.M. from Tom F. Petersen, the NIH and the NSF, and by the Simons Foundation Autism Research Initiative to L.-H.T. K.D. was supported by the NIH Pioneer Program. L.-H.T. is an Investigator of the Howard Hughes Medical Institute. J.A.C. was supported by a K99 from the NIH/NEI; M.C. and K.M. by postdoctoral fellowships from the Knut och Alice Wallenberg Foundation; M.C. by a NARSAD Young Investigator Award; and F.Z. by an NIH NRSA.

References

1. Ascoli GA, et al. Petilla terminology: nomenclature of features of GABAergic interneurons of the cerebral cortex. *Nat Rev Neurosci.* 2008; 9:557–568. [PubMed: 18568015]
2. Connors BW, Gutnick MJ, Prince DA. Electrophysiological properties of neocortical neurons *in vitro*. *J Neurophysiol.* 1982; 48:1302–1320. [PubMed: 6296328]
3. Kawaguchi Y, Kubota Y. GABAergic cell subtypes and their synaptic connections in rat frontal cortex. *Cereb Cortex.* 1997; 7:476–486. [PubMed: 9276173]
4. Markram H, et al. Interneurons of the neocortical inhibitory system. *Nat Rev Neurosci.* 2004; 5:793–807. [PubMed: 15378039]
5. McCormick DA, Connors BW, Lighthall JW, Prince DA. Comparative electrophysiology of pyramidal and sparsely spiny stellate neurons of the neocortex. *J Neurophysiol.* 1985; 54:782–806. [PubMed: 2999347]

6. Kuhlman SJ, Huang ZJ. High-resolution labeling and functional manipulation of specific neuron types in mouse brain by Cre-activated viral gene expression. *PLoS ONE*. 2008; 3:e2005. [PubMed: 18414675]
7. Boyden ES, Zhang F, Bamberg E, Nagel G, Deisseroth K. Millisecond-timescale, genetically targeted optical control of neural activity. *Nat Neurosci*. 2005; 8:1263–1268. [PubMed: 16116447]
8. Sohal VS, Zhang F, Yizhar O, Deisseroth K. Parvalbumin neurons and gamma rhythms enhance cortical circuit performance. *Nature*. 2009; 459:698–702. [PubMed: 19396159]
9. Petreanu L, Huber D, Sobczyk A, Svoboda K. Channelrhodopsin-2-assisted circuit mapping of long-range callosal projections. *Nat Neurosci*. 2007; 10:663–668. [PubMed: 17435752]
10. Petreanu L, Mao T, Sternson SM, Svoboda K. The subcellular organization of neocortical excitatory connections. *Nature*. 2009; 457:1142–1145. [PubMed: 19151697]
11. Tsai HC, et al. Phasic firing in dopaminergic neurons is sufficient for behavioral conditioning. *Science*. 2009; 324:1080–1084. [PubMed: 19389999]
12. Cardin JA, et al. Driving fast-spiking cells induces gamma rhythm and controls sensory responses. *Nature*. 2009; 459:663–667. [PubMed: 19396156]
13. Han X, et al. Millisecond-timescale optical control of neural dynamics in the nonhuman primate brain. *Neuron*. 2009; 62:191–198. [PubMed: 19409264]
14. Huber D, et al. Sparse optical microstimulation in barrel cortex drives learned behaviour in freely moving mice. *Nature*. 2008; 451:61–64. [PubMed: 18094685]
15. Gradinaru V, Mogri M, Thompson KR, Henderson JM, Deisseroth K. Optical deconstruction of parkinsonian neural circuitry. *Science*. 2009; 324:354–359. [PubMed: 19299587]
16. Arenkiel BR, et al. *In vivo* light-induced activation of neural circuitry in transgenic mice expressing channelrhodopsin-2. *Neuron*. 2007; 54:205–218. [PubMed: 17442243]
17. Marin O, Rubenstein JL. Cell migration in the forebrain. *Annu Rev Neurosci*. 2003; 26:441–483. [PubMed: 12626695]
18. Wonders C, Anderson SA. Cortical interneurons and their origins. *Neuroscientist*. 2005; 11:199–205. [PubMed: 15911869]
19. Saito T, Nakatsuji N. Efficient gene transfer into the embryonic mouse brain using *in vivo* electroporation. *Dev Biol*. 2001; 240:237–246. [PubMed: 11784059]
20. Tabata H, Nakajima K. Efficient *in utero* gene transfer system to the developing mouse brain using electroporation: visualization of neuronal migration in the developing cortex. *Neuroscience*. 2001; 103:865–872. [PubMed: 11301197]
21. Tabata H, Nakajima K. Neurons tend to stop migration and differentiate along the cortical internal plexiform zones in the Reelin signal-deficient mice. *J Neurosci Res*. 2002; 69:723–730. [PubMed: 12205665]
22. Tabata H, Nakajima K. Multipolar migration: the third mode of radial neuronal migration in the developing cerebral cortex. *J Neurosci*. 2003; 23:9996–10001. [PubMed: 14602813]
23. Borrell V, Yoshimura Y, Callaway EM. Targeted gene delivery to telencephalic inhibitory neurons by directional *in utero* electroporation. *J Neurosci Methods*. 2005; 143:151–158. [PubMed: 15814147]
24. Taymans JM, et al. Comparative analysis of adeno-associated viral vector serotypes 1, 2, 5, 7, and 8 in mouse brain. *Hum Gene Ther*. 2007; 18:195–206. [PubMed: 17343566]
25. Nathanson JL, Yanagawa Y, Obata K, Callaway EM. Preferential labeling of inhibitory and excitatory cortical neurons by endogenous tropism of adeno-associated virus and lentivirus vectors. *Neuroscience*. 2009; 161:441–450. [PubMed: 19318117]
26. Atasoy D, Aponte Y, Su HH, Sternson SM. A FLEX switch targets Channelrhodopsin-2 to multiple cell types for imaging and long-range circuit mapping. *J Neurosci*. 2008; 28:7025–7030. [PubMed: 18614669]
27. Livet J, et al. Transgenic strategies for combinatorial expression of fluorescent proteins in the nervous system. *Nature*. 2007; 450:56–62. [PubMed: 17972876]
28. Fu H, et al. Self-complementary adeno-associated virus serotype 2 vector: global distribution and broad dispersion of AAV-mediated transgene expression in mouse brain. *Mol Ther*. 2003; 8:911–917. [PubMed: 14664793]

29. Van Vliet KM, Blouin V, Brument N, Agbandje-McKenna M, Snyder RO. The role of the adeno-associated virus capsid in gene transfer. *Methods Mol Biol.* 2008; 437:51–91. [PubMed: 18369962]
30. Jasnow AM, Rainnie DG, Maguschak KA, Chhatwal JP, Ressler KJ. Construction of cell-type specific promoter lentiviruses for optically guiding electrophysiological recordings and for targeted gene delivery. *Methods Mol Biol.* 2009; 515:199–213. [PubMed: 19378132]
31. Tenenbaum L, et al. Recombinant AAV-mediated gene delivery to the central nervous system. *J Gene Med.* 2004; 6 (Suppl 1):S212–S222. [PubMed: 14978764]
32. Aravanis AM, et al. An optical neural interface: *in vivo* control of rodent motor cortex with integrated fiberoptic and optogenetic technology. *J Neural Eng.* 2007; 4:S143–S156. [PubMed: 17873414]
33. Ayling OG, Harrison TC, Boyd JD, Goroshkov A, Murphy TH. Automated light-based mapping of motor cortex by photoactivation of channelrhodopsin-2 transgenic mice. *Nat Methods.* 2009; 6:219–224. [PubMed: 19219033]

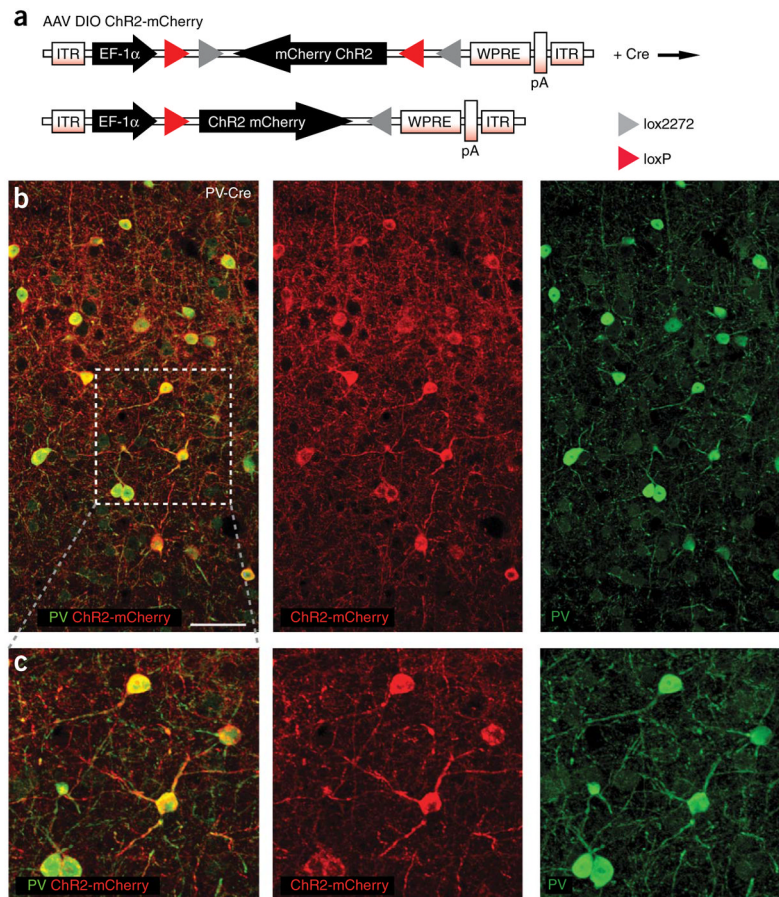


Figure 1. AAV DIO ChR2-mCherry gives Cre-dependent and cell-type-specific expression of light-activated channels *in vivo*. (a) The adeno-associated viral vector AAV DIO ChR2-mCherry carries an inverted version of *ChR2* fused to the fluorescent marker *mCherry*^{8,12}. This strategy prevents *ChR2* from being expressed in the absence of Cre. In the presence of Cre, *ChR2-mCherry* is inverted into the sense direction and expressed from the *EF-1 α* (*EEF1A1*) promoter. EF-1 α , elongation factor 1 α promoter; ITR, inverted terminal repeat; pA, poly(A); WPRE, woodchuck hepatitis B virus post-transcriptional element. (b) ChR2-mCherry (red) is expressed specifically in PV⁺ interneurons (green) 6 d after injection of AAV DIO ChR2-mCherry into the barrel cortex of an adult PV-Cre mouse. Confocal Z-stack of two adjacent 3 μ m sections. Boxed area is shown in higher magnification and detail in c. (c) PV⁺ cells with ChR2-mCherry expression and typical interneuron morphology. Confocal Z-stack of four adjacent 3 μ m sections. Bar = 100 μ m (b). All procedures were conducted in accordance with the National Institutes of Health guidelines and with the approval of the Committee on Animal Care at MIT.

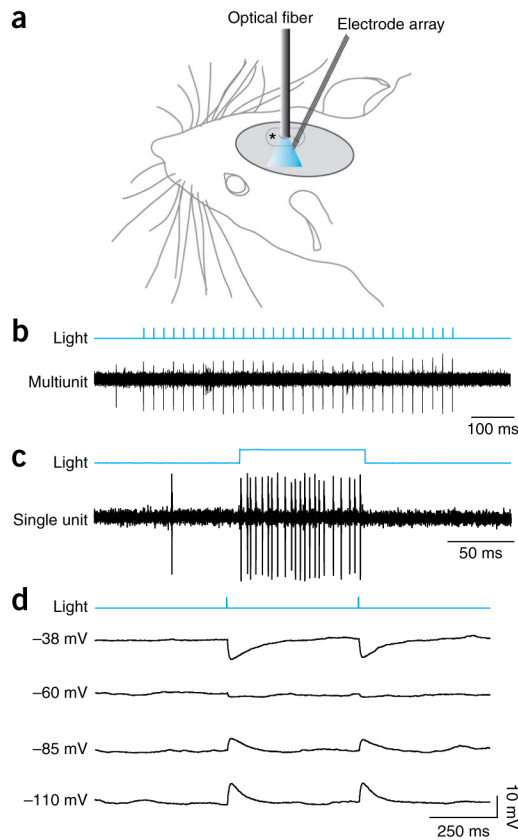


Figure 2. Neural activity evoked *in vivo* by activation of cell-type-specific expression of ChR2. **(a)** Schematic of the placement of the unjacketed optical fiber and extracellular electrode array within the craniotomy (dashed line). Both the optical fiber and the electrodes were placed several hundred micrometers from the original virus injection site (asterisk). **(b)** Individual 1-ms pulses of 473 nm light at 46 mW mm^{-2} through the optical fiber reliably evoked a single action potential from a fast-spiking, PV^+ inhibitory interneuron in the primary somatosensory cortex in this multiunit recording. **(c)** A 100-ms light pulse at the same power level evoked a sustained period of elevated firing ($\sim 220 \text{ Hz}$) from a fast-spiking interneuron in this single-unit recording. **(d)** ChR2 can also be used in conjunction with intracellular recordings *in vivo*. The traces show the membrane potential of a regular spiking, putative excitatory neuron in a PV-Cre mouse expressing ChR2 in fast-spiking inhibitory interneurons. Local inhibitory interneurons were repeatedly stimulated with 1-ms light pulses while the regular spiking cell was held at varying membrane potentials. The inhibitory post-synaptic potentials (IPSPs) resulting from light-evoked activation of presynaptic inhibitory interneurons reversed around -70 mV , indicating a fast, GABA_{A} -mediated chloride conductance.

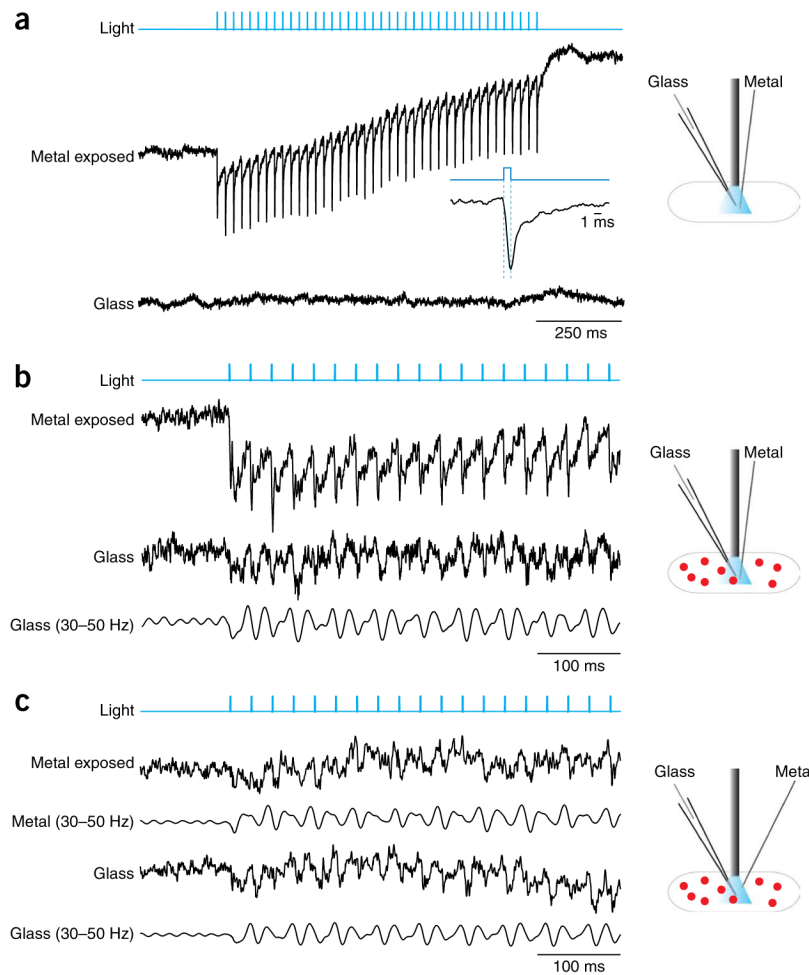


Figure 3. Elimination of light-induced artifacts in recordings of the local field potential. **(a)** Direct exposure of metal electrodes to the laser beam causes large electrical artifacts. These examples are taken from recordings in a cortical site not transduced with AAV-DIO-ChR2-mCherry. A glass pipette with a nonreflective coating was placed in the superficial cortex $\sim 350 \mu\text{m}$ away from a tungsten electrode. The shaft and exposed tip of the tungsten electrode were directly in the cone of blue light, as shown by the schematic to the right. Under these conditions, pulses of laser light (68 mW mm^{-2} ; blue trace) caused a large, repeated artifact in the LFP recording from the metal electrode (upper black trace). The artifact started at the onset of each light pulse and lasted at least 8 ms after the end of the light pulse (see inset). Simultaneous recordings from a glass pipette whose shaft was in the light cone under the optical fiber did not show any light-induced artifacts (lower black trace). **(b)** Similar artifacts were observed when the LFP was recorded from a cortical site containing interneurons transduced with AAV DIO ChR2-mCherry (red dots). In this case, the LFP recorded on the metal electrode shows a gamma oscillation induced by stimulating the fast-spiking interneurons at 40 Hz, but the oscillation signal is obscured by the light-induced artifact caused by the shaft of the metal electrode intersecting the laser beam (upper trace). In contrast, the simultaneous recording from the glass electrode shows the gamma oscillation in the absence of the artifact (middle trace), as highlighted by the filtered glass electrode LFP (lower trace). **(c)** Artifacts in the metal electrode recordings can be eliminated by changing the angle of the electrode so that the shaft does not intersect the laser beam, as

shown in the schematic to the right. In this example, the signal on the angled metal electrode (upper traces) agrees well with the signal on the glass electrode (lower traces).